Extended Non-Singular Terminal Sliding Mode Observer for Sensorless Control of Surface Mount Permanent Magnet Synchronous Motor

Ganapathy Ram A, Santha KR
Department of Electrical & Electronics Engineering, Sri Venketeswara College of Engineering,
Sriperumbudur, India, 602117,
sagraman@gmail.com
santha@svce.ac.in

Abstract: *This paper presents a sliding mode observer for estimating the back emf and thereby, position and speed of a permanent magnet synchronous motor to achieve sensorless drive system. Sliding mode observer design consists of sliding surface, controller design guarantying the sliding mode existence. Extended non-singular terminal sliding surface is a superset of conventional non-singular terminal sliding surface, which guarantee the convergence of system state to zero in finite time. It also overcomes the restriction on the range of the exponent of a power function, of non-singular sliding surfaces, whose exponent is a rational number with positive odd numerator and denominator, with the exponent of power function being a positive real number. The stability of the proposed observer is verified using Lyapunov second method and the validity of the observer is demonstrated by simulation and verified by experimental results.*

Key words: *Surface mount Permanent magnet synchronous motor, Sliding mode observer, Sensorless control*

1. Introduction

The Permanent Magnet Synchronous Motor has been widely used in many industrial applications because of its high efficiency, maintenance free operation and high controllability. Since PMSM receives a sinusoidal flux from the permanent magnet of the rotor, precise position data are necessary for an efficient vector control. Generally, the rotor position can be detected by a resolver or by an absolute encoder. As an important application of PMSM, the motion control not only requires the accurate rotor position for field orientation but also the information of rotor speed for closed loop control. Cost and volume reduction, wires removal and increased reliability are in favour of position sensorless control of PMSM drives [1], using estimation of the rotor position.

Nowadays, Field Programmable Gate Array's (FPGAs) have become more effective as they allow the implementation of complex control strategies. Earlier, Digital Signal Processor's were used [2], which made the sensorless control technique of PMSM possible. At present, the sensorless control technology can mainly be classified into two types: the estimation method based on observer [3-7] and the high frequency injection method using the salient effect of motor [8-11]. The estimation based method based on observer relies on the accuracy of the motor model to some extent whereas high frequency injection method is independent of the motor model. But, the high frequency signal injection brings high frequency noise, leading to system performance degradation. Given the aforementioned circumstances, the sliding mode observer (SMO) is used because of its simple algorithm and robustness, which makes up for the dependence of observer on the model to a certain extent. The SMO maintains good robustness of variable structure control [12-14].

The control loop in an ordinary observer is replaced by a sliding mode variable structure, and when the system error reaches the sliding mode, the system dynamic performance depends entirely on sliding surface, which ensures good robustness of the entire system to parameter variations. The fundamental design procedure of the sliding mode control is to design a stable sliding surface s, satisfying the desired specifications, and design a feedback control law u which is discontinuous, such that the sliding surface could be reached and retained in the sense of Lyapunov, despite the presence of modeling uncertainties and disturbances.

This paper is organized as follows. The mathematical model of PMSM is reviewed in Section 2. Conventional sliding mode observer is presented in Section 3. New sliding mode observer is proposed in Section 4. Estimation of rotor position and speed is given in Section 5 .System configuration is given in Section 6. Section 7 is presented with simulation and experimental results. Some conclusions are given in Section 8.

2. Mathematical Model of Pmsm

BUPT

The dynamic equations of a PMSM without saliency in the stationary reference frame [15] can be expressed as follows,

$$L_s\left(\frac{di_\alpha}{dt}\right) = -R_s i_\alpha - e_\alpha + u_\alpha \quad (1)$$

$$L_s\left(\frac{di_\beta}{dt}\right) = -R_s i_\beta - e_\beta + u_\beta \quad (2)$$

$$e_\alpha = -\psi_f \omega_r \sin\theta \quad (3)$$

$$e_\beta = \psi_f \omega_r \cos\theta \quad (4)$$

$$e_\beta = \psi_f \omega_r \cos\theta$$

where i_α, i_β, u_α, u_β, and e_α, e_β are the phase currents, phase voltages, and back EMF in the stationary reference frame, respectively, R_s is the stator phase resistance, L_s is the stator phase inductance, ψ_f is the flux linkage of the permanent magnet, ω_r is the electrical angular velocity, and θ is the electrical rotor position. The relation between the stator coordinates and the synchronous coordinates is graphically represented in Fig. 1.

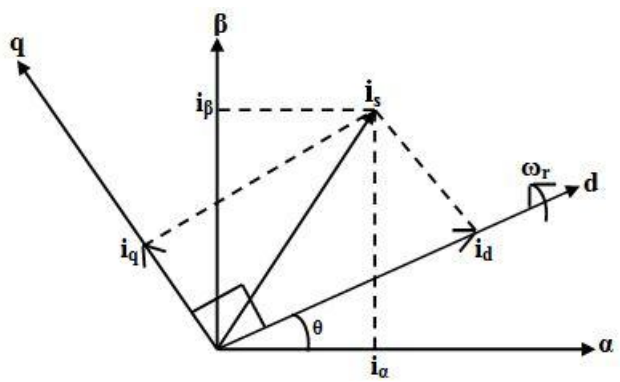


Fig.1. Relation between stator reference coordinates and synchronous rotating coordinates systems.

It can be seen from the back EMF function in (3) and (4) that the back EMF signal contains the information of rotor speed and position. Therefore, after the back EMF signal is estimated by using the observer, the information of rotor speed and position can be obtained.

3. Conventional sliding mode observer

The sliding mode observer has its base on the variable structure theory. In order to design a sliding mode observer, first a sliding surface has to be defined. The sliding surface [15] is defined as,

$$s(x) = \hat{i}_s - i_s \quad (5)$$

where $\hat{i}_s = [\hat{i}_\alpha \quad \hat{i}_\beta]$ is the estimated value of current and $i_s = [i_\alpha \quad i_\beta]$ is its measured value.

With reference to the mathematical model of PMSM in the stationary reference frame, the equations governing sliding mode observer is expressed as follows,

$$L_s\left(\frac{d\hat{i}_\alpha}{dt}\right) = -R_s \hat{i}_s + u_\alpha - KF(\hat{i}_\alpha - i_\alpha) \quad (6)$$

$$L_s\left(\frac{d\hat{i}_\beta}{dt}\right) = -R_s \hat{i}_s + u_\beta - KF(\hat{i}_\beta - i_\beta) \quad (7)$$

$$F(x) = \left[\frac{2}{(1+e^{-ax})}\right] - 1 \quad (8)$$

where 'a' is an adjustable parameter and k is the observer gain. In equation (6) and (7) signum function is replaced with sigmoid function [15], by which the switching between 0 and 1 will be smooth so that the effect of chattering will be very less and hence the requirement of a low pass filter at the output and its phase angle compensation requirement can be avoided. Speed and position of the rotor can be estimated with the help of this observer. The output of this sliding mode observer will be back emfs of the machine in the stationary reference frame. This can be employed to estimate the speed and position as follows,

$$\widehat{\omega_e} = \frac{(\sqrt{\widehat{e_\alpha}^2 + \widehat{e_\beta}^2})}{\psi} \quad (9)$$

and speed is integrated to obtain position.

4. Proposed sliding mode observer

A complete survey of SMO design methods is introduced in [7] and [16]. Among these methods, the so called terminal sliding mode (TSM) control [3] proposed a non linear sliding surface that guarantees the reachability of the sliding mode s=0 in finite time, which is a significant improvement in comparison with the conventional sliding mode control of linear sliding surface, which only ensures asymptotical convergence of *s* [6]. During the control design of fast terminal sliding mode controllers, there often exists a singularity problem. The reason is that the designed controllers have non-linear terms which results in the unboundedness of the control input when the state

BUPT

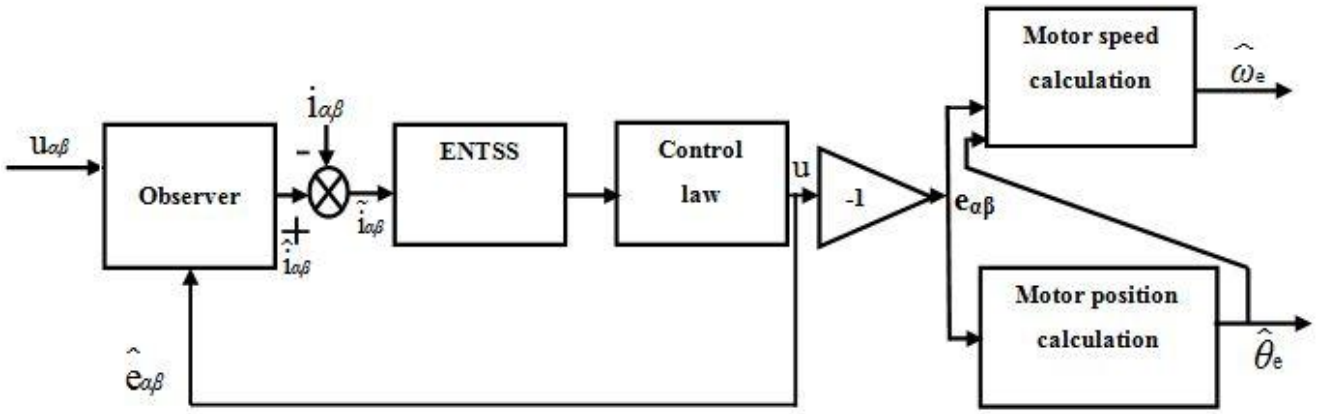


Fig. 2. Structure of proposed SMO.

variable diminishes to zero [10]. Here, the state variables refer to stator currents in stationary frame.

The structure of proposed sliding mode observer is shown in Fig 2. In Fig.2, current observer is supplied with transformed two phase voltage. Output of the observer is estimated current and the error between the actual, estimated current is given as input to the extended non singular terminal sliding surface, ensuring error is zero. Control law maintains the error being kept in zero. Control signal, which is also the the estimated back emf is feedback to the observer ensuring the stability of observer in closed loop operation of sensorless control system shown in Fig.3. With the estimated back EMF, rotor position and speed is calculated. Conventional terminal sliding mode controllers use terminal sliding surfaces, designed using a power function of a system state which guarantee the system state reaching zero in finite time. However, the surfaces suffer from singularity problem and have restrictions on the range of the exponent of a power function. The exponent should be a rational number with positive odd numerator and denominator [17].

To overcome the restrictions on the range of the exponent of power function and singularity problem, the non-singular terminal sliding surface (s_n) is proposed [18] as,

$$s_n = [s_\alpha \quad s_\beta] \tag{10}$$

$$s_\alpha = \left|\dot{\bar{i}}_\alpha\right|^{\frac{1}{p}} \operatorname{sgn}(\bar{i}_\alpha) + c\bar{i}_\alpha \tag{11a}$$

$$s_\alpha = \left|\dot{\bar{i}}_\beta\right|^{\frac{1}{p}} \operatorname{sgn}(\bar{i}_\beta) + c\bar{i}_\beta \tag{11b}$$

where, $\bar{i}_\alpha = \hat{i}_\alpha - i_\alpha$, $\bar{i}_\beta = \hat{i}_\beta - i_\beta$ and $\dot{\bar{i}}_\alpha$, $\dot{\bar{i}}_\beta$ represent the current errors and derivatives of current errors of the stator current in stationary frame. Also sgn(.) is the signum function, C is a positive constant, and ½ ≤ p < 1 is a real number. . For the system (1) and (2) the following controller [18] guarantees that the sliding mode condition holds:

$$u_1 = \frac{J}{(\frac{3}{2}np\psi)}\left(-R_s\bar{i}_\alpha - cp\left|\dot{\bar{i}}_\alpha\right|^{(2-(\frac{1}{p}))} \operatorname{sgn}(\dot{\bar{i}}_\alpha) - k_1(s_\alpha) - k_2\operatorname{sgn}(s_\alpha)\right)$$

(12a)

$$u_2 = \frac{J}{(\frac{3}{2}np\psi)}\left(-R_s\bar{i}_\beta - cp\left|\dot{\bar{i}}_\beta\right|^{(2-(\frac{1}{p}))} \operatorname{sgn}(\dot{\bar{i}}_\beta) - k1(s_\beta) - k2\operatorname{sgn}(s_\beta)\right)$$

(12b)

where, $[u_1 \quad u_2] = [\hat{e}_\alpha \quad \hat{e}_\beta]$ are the estimated back emf's and $k_1>0$, $k_2> \left|\frac{\frac{3}{2}np\psi}{J}\right|(d+\alpha)$ d – load torque(disturbance) with α – being a positive constant.

BUPT

5. Estimation of rotor position and speed

The non-singular terminal sliding surface (s_n) is used to realize the second order sliding-mode control. After s_n reaches zero in finite time, both estimated current and its derivative will reach zero in finite time and stay on the second-order sliding mode. From (12a and 12b), utilizing the second-order sliding mode, back EMF is estimated:

$$\hat{\theta}_e = \arctan\left(\frac{\hat{e}_\alpha}{\hat{e}_\beta}\right) \tag{13}$$

$$\hat{\omega}_e = \left(\frac{\sqrt{\hat{e}_\alpha^2 + \hat{e}_\beta^2}}{\psi}\right)\mathrm{sgn}(\hat{e}_\alpha \cos\hat{\theta}_e - \hat{e}_\beta \sin\hat{\theta}_e) \tag{14}$$

where, $\hat{\theta}_e$ -estimated rotor position, $\hat{\omega}_e$ - estimated speed, ψ - rotor flux.

Finally, from (13) and (14) rotor position and speed is calculated.

6. System configuration

The PMSM is modeled in three-phase stationary coordinates, and is transformed into the (d,q) two-phase synchronous coordinates system for vector control. In the control of speed and current references, the PI control is used to effectively reduce the accumulative errors. The current is supplied to the stator of the motor through the SVPWM control in the form of sinusoid. Using the estimated position and velocity of the rotor, the closed loop sensorless control of the motor is implemented. The specifications of the SMPMSM utilized in this research are listed in table 1. Fig.3 shows the block diagram of the sliding mode observer based sensorless speed control system. Using the estimated position and velocity of the rotor, the closed sensorless control of the motor is implemented.

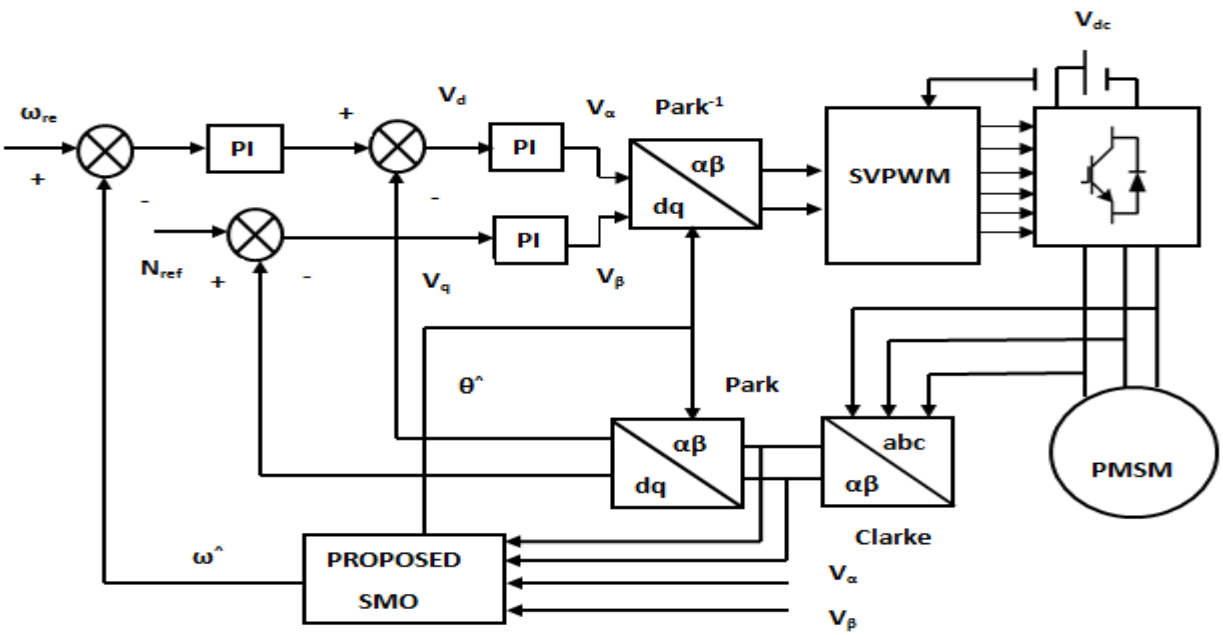


Fig . 3. Block Diagram of proposed sensorless speed control system.

7. Simulation and experimental results

Simulation is carried on MATLAB / SIMULINK environment to validate the proposed observer, with the specifications of SMPMSM in table 1.

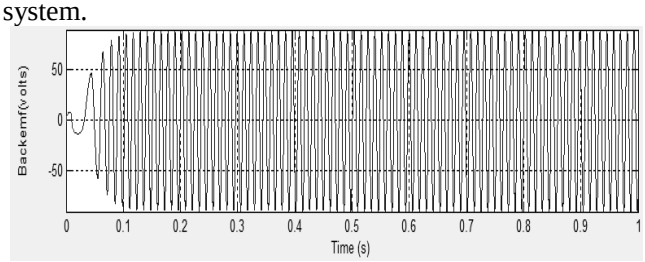


Fig.4.a. Back EMF obtained from observer.

BUPT

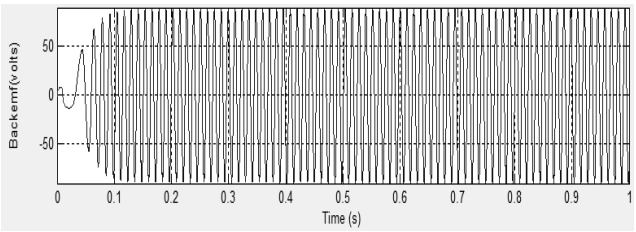


Fig.4.b. Back EMF obtained from observer.

Back EMF, ealpha and ebeta obtained by simulation is shown in Fig. 4.a and Fig .4.b.

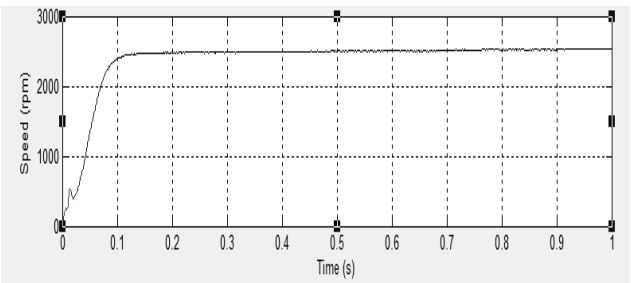


Fig.5. Estimated speed.

Estimated speed is shown in Fig. 5. Speed reference is set as 2500 rpm, and set value is tracked attaining steady state in 0.15seconds.

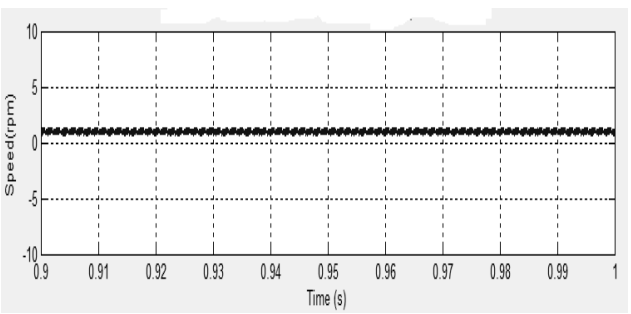


Fig.6. Speed estimation error.

Fig.6. Shows speed estimation error which is less than 5 rpm.

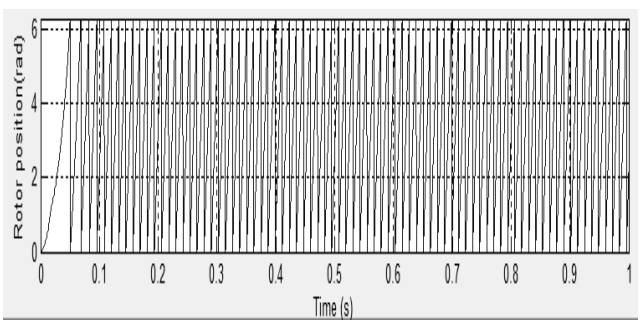


Fig.7. Estimated rotor position.

Fig.7. shows estimated rotor position in radians.

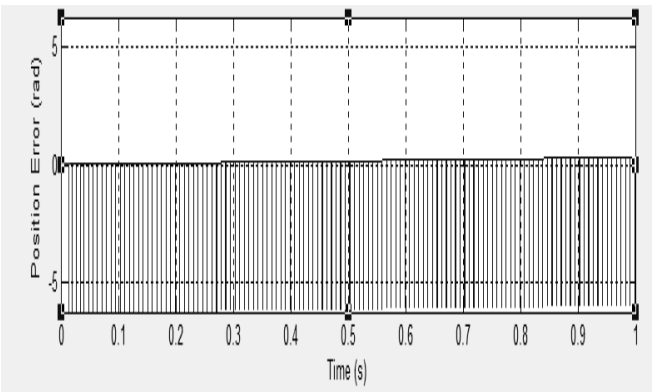


Fig.8. Position Estimation Error.

Fig 8. Shows position estimation error which is nearly zero.

Simulation results are verified experimentally in the laboratory environment. SMPMSM with the specifications listed on table one is used with intelligent power module, PEC16DSM01, rated 25A and 1200V supplying the setup. XILINX VPE SPARTAN 6 AD is the digital controller used. In the experiment, instead of maximum torque per ampere operation, q-axis current command is generated from the speed control loop and d-axis current command is set to zero. The sampling period for current control and rotor position estimation is chosen to be 0.1ms, and the switching frequency of the PWM inverter is 10 kHz. The space vector PWM algorithm was applied and updated every 100 μs with respect to switching frequency. Fig. 9. shows the experimental setup. To control the PMSM, the three-phase coordinates need to be transformed into *d–q* synchronous coordinates, which are a part of the vector control. As a result of the vector control, a reference current is generated and passed to the stator of the motor through the inverter. Using the error between the command and estimated speed, the proportional–integral (PI) control is implemented, which is also used for the current control.

BUPT

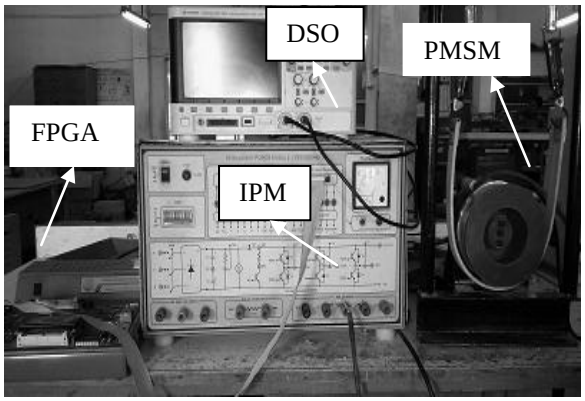


Fig.9. Experimental setup.

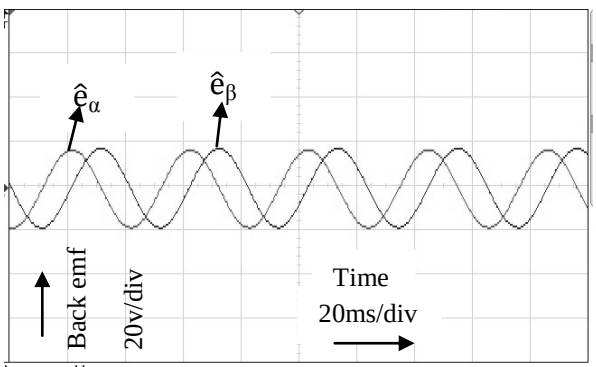


Fig.10. Back EMF obtained experimentally.

Fig.10 shows back EMF values estimated in stationary reference frame. Back EMF waveforms obtained appear sinusoidal, which is by the design of motor itself.

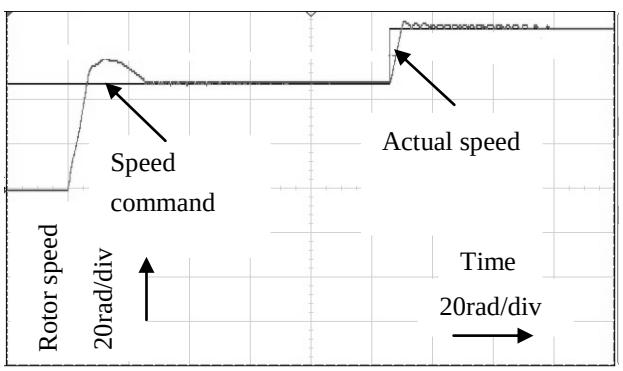


Fig.11. Speed with step change.

Fig.11 shows speed, which tracks the set value of 42 radians per second and responds to the step change attaining the value of 60 radians per seconds.

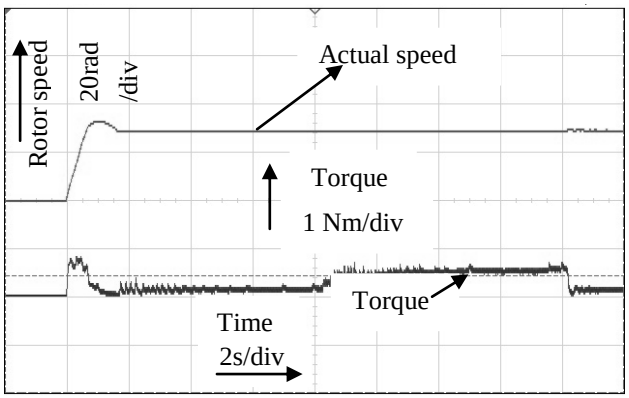


Fig.12. Speed and torque.

Fig.12 shows the variation in torque to the step change. When, step change is applied at 10s, torque changes and attains steady state at 18s.

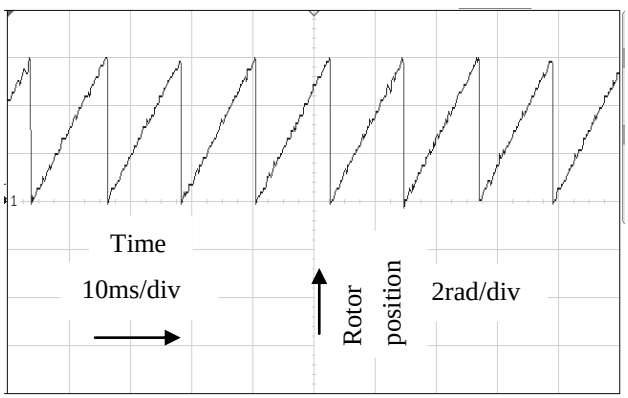


Fig.13. Rotor position.

Fig.13 shows the rotor position in radians.

Table 1

Parameters of tested pmsm

Number of pole pairs	2
Rated speed	4600 rpm
Armature resistance R_a	3.07Ω
d-axis inductance L_d	$6.57X10^{-3}$ mH
q-axis inductance L_q	$6.57X10^{-3}$ mH
Flux of permanent magnet	0.2 Wb
Rated torque	2.2 Nm

7 . Conclusions

An Extended non-singular terminal sliding mode observer is designed. Proposed design overcomes

BUPT

restriction on exponent of power function being rational with positive odd numerator and denominator in the sliding surface design by extending with positive real number. Back EMF estimated from observer is used to calculate rotor position and speed of Permanent Magnet Synchronous Motor. From the experimental results it can be observed that the operation of vector control system with proposed observer is satisfactory.

Appendix

Proof of the stability[18] of the proposed SMO:

Let the Lyapunov candidate be:

$$V(s) = \frac{1}{2} x s^2$$

from (1), (2) and (12a), (12b) $\frac{dv}{dt} = \dot{V}$, the following equations can be obtained if:

$\dot{i}_s > 0$; that $i_s < 0$:

$$\dot{V}(s) = s\dot{s} = s(\frac{1}{p}\dot{i}_s^{((\frac{1}{p})-1)}\ddot{i}_s + c\dot{i}_s)$$

$$\leq s(\frac{1}{p}\dot{i}_s^{((\frac{1}{p})-1)})(-k_1 s - \alpha \operatorname{sgn}(s))$$

$$(\frac{1}{p}\dot{i}_s^{((\frac{1}{p})-1)}(R_s + (1.5 * np * \psi / J)) + c\dot{i}_s)$$

$$\leq (\frac{1}{p}i_s^{((\frac{1}{p})-1)})(-k_1 s^2 - \alpha(|s|) \quad (1)$$

similarly, if $\dot{i}_s < 0$; that $i_s > 0$:

$$\dot{V}(s) = s\dot{s} = s(\frac{1}{p}(-\dot{i}_s)^{((\frac{1}{p})-1)}\ddot{i}_s + c\dot{i}_s)$$

$$\leq s(\frac{1}{p}\dot{i}_s^{((\frac{1}{p})-1)})(-k_1 s - \alpha \operatorname{sgn}(s))$$

$$(\frac{1}{p}(-\dot{i}_s)^{((\frac{1}{p})-1)}(R_s + (1.5 * np * \psi / J)) + c\dot{i}_s)$$

$$\leq (\frac{1}{p}(-i_s)^{((\frac{1}{p})-1)})(-k_1 s^2 - \alpha(|s|)$$

(2)

equations (1) and (2) can be represented as

$$\dot{V}_s = -\frac{1}{p}\left|\dot{i}_s\right|^{((\frac{1}{p})-1)}(k_1 s^2 + \alpha|s|)$$

here $\dot{V}(s) < 0$ if $i_s \neq 0$ and $s \neq 0$ (3)

if $\left|\dot{i}_s\right| = 0$, from (1), (2) and (12), the following equation can be obtained:

$$\ddot{i}_s = \frac{di_s}{dt} = -k_1 s - k_2 \operatorname{sgn}(s) + g.d \quad (4)$$

where $g = \frac{(\frac{3}{2} np\psi)}{J}$, J-moment of inertia of the rotor, ψ -rotor flux and n_p -number of poles.

which implies that:

$$(s\frac{di_s}{dt} \mid \dot{i}_s = 0) \leq -k_1 s^2 - \alpha|s| \quad (5)$$

Thus, it is clear that if $|i_s| = 0$ and $s \neq 0$, i_s deviates from zero; that is, the set of points $|i_s| = 0$ and $s \neq 0$, is not an attractor.

In phase space, these points are all points on the horizontal axis that save the origin. Therefore, we can conclude that s goes to zero.

BUPT

References

[1] Young-Seok Jung, Marn-Go Kim, *Sliding Mode Observer for Sensorless control of IPMSM Drives*. In: Journal of Power Electronics, Vol. 9, no. 1, 2009 , pp.117-123.

[2] Buccella C, Cecati C, and Latafat H, *Digital control of power converters—A Survey*. In: IEEE Trans. Ind. Informatics., vol. 8, no. 3, August 2012, pp. 437– 447.

[3] Bandyopadhyay B, Janardhanan. S, and Spurgeon S K, *Advances in Sliding Mode Control: Concept, Theory and Implementation*. (Lecture Notes in Control and Information Sciences), vol. 440. Berlin, Germany: Springer, 2013.

[4] Foo G and Rahman M F, *Sensorless sliding-mode MTPA control of an IPM synchronous motor drive using a sliding-mode observer and HF signal injection*. In: IEEE Trans. Ind. Electron., vol. 57, no. 4, April 2010, pp. 1270–1278.

[5] Jang J S et al, *Parallel reduced-order extended Kalman filter for PMSM sensorless drives*. In: in Proceedings of IEEE Industrial Electronics Society Annual Conference, Florida, November 2008, pp. 1326–1331.

[6] Jinchuan Zheng et al, *Robust Motion Control of a Linear Motor Positioner Using Fast Nonsingular Terminal Sliding Mode*. In: IEEE/ASME Transactions on Mechatronics, 2014, pp. 1355–1366.

[7] J E Slotine and W Li, *Applied Nonlinear Control*. Englewood Cliffs, NJ, USA: Prentice-Hall, 1991.

[8] Liu H and Li S, *Speed control for PMSM servo system using predictive functional control and extended state observer*. In: IEEE Trans. Ind. Electronics., vol. 59, no. 2, February 2012, pp. 1171–1183.

[9] Leidhold R, *Position sensorless control of PM synchronous motors based on zero-sequence carrier injection*. In: IEEE Trans. Ind. Electron., vol. 58, December 2011, no. 12, pp. 5371–5379.

[10] Man Z and Yu X, *Terminal sliding mode control of MIMO systems*. In: IEEE Trans. Circuits Syst. I, Fundam. Theory Appl, vol. 44, no. 11, November 1997, pp. 1065–1070.

[11] Orlowska-Kowalska.T and Dybkowski. , M S *Stator-current-based MRAS estimator for a wide range speed-sensorless induction-motor drive*. In: IEEE Trans. Ind. Electron., vol. 57, no. 4, April 2010, pp. 1296–1308.

[12] Pellegrino G, Giangrande P, and Salvatore. L, *Sensorless position control of permanent-magnet motors with pulsating current injection and compensation of motor end effects*. In: IEEE Trans. Ind. Appl., vol. 47, no. 3, May/June 2011, pp. 1371–1379.

[13] Piippo A, Hinkkanen M, and Luomi J, *Analysis of an adaptive observer for sensorless control of interior permanent magnet synchronous motors*. In: IEEE Trans. Ind. Electron., vol. 55, no. 2, February 2008, pp. 570–576.

[14] Sabanovic A, *Variable structure systems with sliding modes in motion control—A survey*. In: IEEE Trans. Ind. Informatics., vol. 7, no. 2, May 2011, pp. 212–223.

[15] Kim H, Son J, Lee J. *A high-speed sliding-mode observer for the sensorless speed control of a PMSM*. In: IEEE Transactions on Industrial Electronics, Vol 58(9), 2011, 4069–77.

[16] V I Utkin, *Sliding Modes in Control and Optimization*. New York, NY, USA: Springer-Verlag, 1992.

[17] Yang L and Yang, *Nonsingular fast terminal sliding-mode control for nonlinear dynamical systems*. In: International Journal of Robust and Nonlinear Control, vol. 21, no. 16, January 2011, pp. 1865–1879.

[18] Ji wung Jeong, Ho Suk Yeon, Kang Bak Park, Extended Nonsingular terminal sliding surface for second order nonlinear systems. In: Abstract and Applied Analysis, May 2014.

Biographies

A. Ganapathy Ram received his B.E., degree in Electrical and Electronics Engineering from Madras University, India and Masters in Applied Electronics from Bharath University, India. Currently he is working towards his Ph.D degree. His research interests are in the areas of Sensorless Control, Special Electrical Machines.

KR. Santha received her B.E., degree in Electronics and Instrumentation from Annamalai University, India, her Master's in Control systems from Osmania University, India and Ph.D., from Madras Institute of technology, Chennai, India. She is working as Professor and Head of the Department of Electrical and Electronics Engineering in Sri Venkateswara College of Engineering, Chennai, India. Her research interests are in the areas of Discrete time systems and Signal Processing, High speed VLSI Architectures and Asynchronous Circuits.